IRS Observations of PAHs and CO_2 Ice in the Galactic Center

Janet P. Simpson[1,2]

ABSTRACT

During Cycle 1 we used Spitzer to take high-res IRS spectra (10 - 38 μm) of 38 positions in the Galactic Center (GC), all at the same Galactic longitude of and including the Arches Cluster. Our positions include the Arched Filaments, regions near the Quintuplet Cluster, the "Bubble" south of the Quintuplet Cluster, and the diffuse interstellar gas along the line of sight at higher Galactic latitudes. From the line fluxes measured from our GC spectra we determined that the Arched Filaments appear to be H II regions excited by the Arches Cluster and that the Bubble contains significant amounts of shocked gas, probably as a result of the winds from the massive stars of the Quintuplet Cluster (Simpson et al. 2007). Here we present our analysis of the continuum features seen in these spectra. Just as the lines show that there are substantial differences in the local environment with position in the GC (e.g., density, excitation, radiation field, amount of shocked gas), the polycyclic aromatic hydrocarbon features (PAHs) show widely varying ratios with respect to the continuum emission, being strongest for sight lines through the diffuse ISM at 0.3 degrees distance from the Galactic plane but having small equivalent widths in the high-continuum Arched Filaments. In our Short-High spectra these features occur at 11.0, 11.2, 12.0, 12.6, 13.5, 14.2, and 16.3 - 17.5 μm. Finally, a few positions in the Arched Filaments and the G0.099-0.166 radio and infrared source (probably an ultra-compact H II region) exhibit the 15.2 μm CO2 ice feature. We discuss the correlations of these features with each other and with their local environments as previously determined from the line measurements.

Subject headings: Galaxy: center — dust, extinction — H II Regions — infrared: ISM — ISM: lines and bands — ISM: molecules

[1]NASA Ames Research Center

[2]SETI Institute

1. Introduction

Spectra of the mid-infrared (MIR) emission features commonly thought to be due to polycyclic aromatic hydrocarbon molecules (PAHs) are observed to be variable with type of source and position within a source. For example, the 6.2, 7.7, and 11.2 μm features can be sorted into three classes depending on the wavelength of the peak emission of the feature (Peeters et al. 2002; van Diedenhoven et al. 2004; see Peeters et al. 2004a for a review). The 6.2, 7.7, and 11.2 features in class A peak at the shortest wavelength; typical sources include H II regions, star forming galaxies, and reflection nebulae. Classes B and C peak at longer wavelengths; sources emitting class B and C features are all evolved stars, AGB stars, or planetary nebulae (note that a few such evolved sources emit class A features instead). Some sources can include features of both classes B and A at different distances from the exciting star (Peeters et al. 2004a). These variations are undoubtedly the result of the molecule formation process and subsequent differences in evolutionary history due to different local environments. Environmental factors can include the intensity of the radiation field, expressed as G_0, the ratio of the ultraviolet (UV, 6 – 13.6 eV) photon density to that of the "local interstellar radiation field", the electron density n_e (G_0/n_e determines the ionization equilibrium), the hardness of the radiation field (extreme UV photons, EUV, or X-rays can dissociate molecules), or the presence of shocks (which can also dissociate molecules).

The spectral region from 10 to 15 μm includes a number of PAH features in addition to the 11.3 μm feature, which are due to CH out-of-plane bending mode vibrations. The 11.2 μm feature is the strongest, but there are others at 11.0, 12.0, 12.6, 13.5, and 14.2 μm, thought to be due to the PAH molecule's charge state (neutral or cation), or the presence of adjacent CH groups (Hudgins & Allamandola 1999; Hony et al. 2001). Additional features can occur in the 16 – 19 μm region. This complex includes emission features at 15.9, 16.4, 17.4, 17.8, and 18.9 μm lying on top of a plateau centered at 17.0 μm. Probably arising from PAH CCC out-of-plane bending vibrations (Peeters et al. 2004b), the features in this complex show substantially more variation than the complex of features from 11 – 14 μm (e.g., the reflection nebula NGC 7023, Sellgren et al. 2007).

With the advent of Spitzer Space Telescope (Werner et al. 2004), spectra of much fainter sources can be investigated with much higher signal/noise than was possible with the Infrared Space Observatory or the Kuiper Airborne Observatory. In Cycle 1 (Program 3295) we obtained spectra of 38 positions towards the Galactic Center (GC; Figure 1) with the Infrared Spectrograph's Short-High (SH) and Long-High (LH) modules (Houck et al. 2004). From the line measurements we are able to characterize the environments seen in the GC and along the lines of sight towards the GC through the diffuse interstellar medium (ISM)

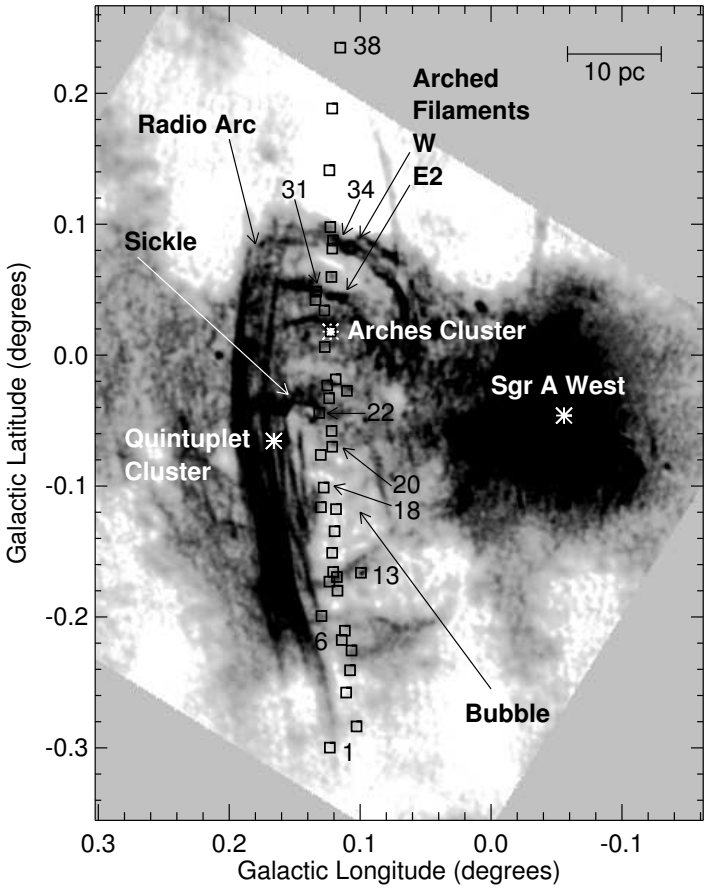

Fig. 1.— Radio continuum (log-log scale) imaged at 21 cm by Yusef-Zadeh & Morris (1987) with 11″ resolution. The observed positions (square boxes) are numbered from 1 to 38, starting at the lowest Galactic latitude. The massive star clusters, Sgr A, Arches, and Quintuplet Clusters, are marked. The Radio Arc and part of the Sgr A region (Sgr A East) are nonthermal; the rest of the continuum is thermal bremsstrahlung.

(Simpson et al. 2007). The lines of sight for all positions include both warm molecular gas, as seen by the strong H_2 lines, and H II regions and PDRs, as seen by the lines from ionized species. The PDR lines ([Si II] and [Fe II]) correlate better with the H II region lines than with the H_2 lines. All positions also include the high excitation [O IV] line, which may be evidence of shocked gas in the diffuse ISM along the line of sight. The Arched Filaments are excited by the Arches Cluster, which must be nearby to them since their [S III] 33.5 μm/[Si II] 34.8 μm line ratios show that the EUV radiation field has the high intensity typical of compact H II regions. The positions near the Quintuplet Cluster, the Sickle Handle, the Bubble, and the Bubble Rim are excited by the Quintuplet Cluster because they show higher excitation than the Arched Filaments, even though the radiation field at those positions is much more dilute than in the Arched Filaments. We attribute the radiation field dilution to being due to the gas lying at substantial distances from the exciting stars. The combination of high excitation

gas and low intensity radiation field can be explained either by the ionizing photons being extremely high energy (X-rays) or by shocks. There is additional evidence for shocks (i.e., shock destruction of grains) in the Bubble in that its gas-phase iron abundance is a factor of 6.5 higher than in the surrounding positions.

In this paper we discuss the effects of environment on the PAH continuum features seen at these positions.

2. Observations

Figure 2 of Simpson et al. (2007) shows three typical spectra from the combined SH and LH wavelength ranges. Since there are no narrow continuum features seen in the LH spectra, we here discuss only the SH spectra (10 – 19.5 μm). Each position was mapped with a 3 by 2 map to include approximately the area covered by the Long-High (LH) slit on the sky. The maps covered 13″ by 14″. Four ramps were taken for each telescope pointing and the resulting basic calibrated data (bcd) images from the S15 pipeline were median-combined and cleaned of bad and rogue pixels. A three-dimensional cube was created from the bcd images and the spectra were extracted using CUBISM (Smith et al. 2007). The sizes of the extraction boxes were 5 by 5 pixels in all cases except for Position 13, which includes the G0.099-0.166 source; here a 3 by 4 box was used to concentrate on the deeply embedded source. Position 28 is a map of the Arches Cluster (made with 3 ramps per pointing), but one edge includes part of the E1 Arched Filament. The spectrum called Position 28 discussed here is a 5 by 5 pixel extraction of that Arched Filament region, not the star cluster.

3. Analysis and Results

For each spectrum, an estimate of the Zodiacal background was subtracted and the spectrum was corrected for extinction (Simpson et al. 2007). The continuum was estimated by fitting a spline through those wavelengths that do not contain the well-defined PAH features (11.2, 12.0, etc.) or CO_2 ice feature (15.2 μm) and subtracted. The resulting spectra from eight positions are shown in Figure 2. We are assuming here that the broad plateau underlying the PAH features between 11 and 15 μm is a distinct feature and should be measured separately. For many of our positions this region includes substantial continuum from warm dust (compare the continuum seen in the three spectra of Fig.2 of Simpson et al. 2007). Equivalent widths of each of the PAH and CO_2 ice features were computed.

For all positions, the shapes of the 11.0, 11.2, 12.0, 12.6, 13.5, and 14.2 μm PAH features

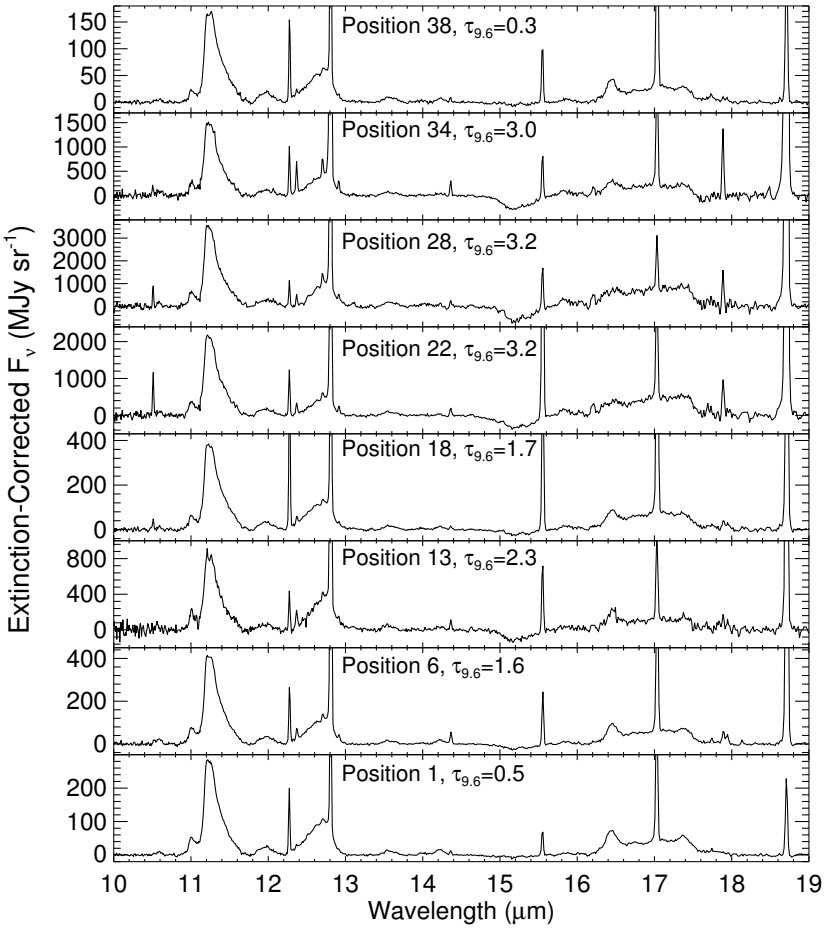

Fig. 2.— Eight Short-High spectra showing the PAH emission and the 15.2 μm CO_2 ice absorption features.

are quite similar, typical of H II region PAHs (class A). (The PAH features in the 6 – 10 μm region are also typical H II region PAHs, Simpson et al. 1999). There is no correlation of the CO_2 15.2 μm ice absorption feature with optical depth at 9.6 μm, $\tau_{9.6}$. The total fluxes integrated over the 17 μm complex correlate almost perfectly with the fluxes in the 11.2 μm PAH feature, from which we conclude that the 17 μm complex is indeed due to PAH emission.

However, even though all the PAH features from 6 – 15 μm are class A and very similar, the 15 – 18 μm region shows differences as a function of environment:

Diffuse warm ISM: Broad 17 μm plateau feature with clearly resolved features at 16.4 μm (very prominent) and 17.4 μm (substantially weaker). Very weak 15.2 μm absorption.

Positions 1, 2, 3, 4, 36, 37, 38.

High-intensity radiation field H II regions: Broad 17 μm plateau feature with *no* obvious 16.4 or 17.4 μm features (the spectra are noisy because the 17 μm continuum is high and the feature/continuum ratio is low). The 15.2 μm CO_2 ice feature is present. Positions 28, 29, 30, and 31 in the Arched Filaments and 22 and 24 in the Sickle Handle.

Medium-intensity radiation field H II regions: Broad 17 μm plateau with noticeable (not prominent) 16.4 μm feature and weak or not detectable 17.4 μm feature. Detectable CO_2 ice feature. Positions 27, 33, and 34 in the Arched Filaments, Positions 23, 25, and 26 in the Sickle Handle, and Positions 19 – 21 in the Bubble.

Low-medium intensity radiation field H II regions: The 16.4 μm feature is very prominent compared to the 17 μm plateau but the 17.4 μm feature is not obvious. Detectable CO_2 ice feature. Positions 10 – 18 in the Bubble and Bubble rim.

Low-intensity radiation field H II regions: The 16.4 μm feature is very prominent compared to the 17 μm plateau and the 17.4 μm feature is obvious. Detectable CO_2 ice feature. Positions 5 – 9 in the Bubble rim farthest from the Quintuplet Cluster and Positions 32 and 35 in the diffuse regions of the Arched Filaments.

Deeply embedded, possible ultracompact H II region: Deepest CO_2 ice feature. Position 13 (G0.099-0.166).

The 17.8 and 18.9 μm features that are prominent in the neutral gas of the NGC 7023 reflection nebula (Sellgren et al. 2007) are not apparent in the ionized gas of the GC.

The environmental parameter affecting PAH ionization is G_0/n_e. The MIR continuum is also affected by G_0 because very small dust grains are stochastically heated (Draine & Li 2007, and references therein). The parameter corresponding to G_0/n_e for the ionization equilibrium of atoms is U, the ratio of the ionizing photon density divided by n_e. H II region model calculations have shown that the [S III] 33.5 μm/[Si II] 34.8 μm line ratio is a good estimator of U for dilute radiation fields (both Si and S are normally doubly ionized, but recombine to Si^+ and S^+ when $\log U \lesssim -2$). One would expect G_0 and U to be correlated, and this is the case, as is shown in Figure 3. We conclude that where the ISM is ionized, the [S III] and [Si II] lines can be used as a proxy in the estimation of the radiation field intensity that heats the dust and excites the PAHs.

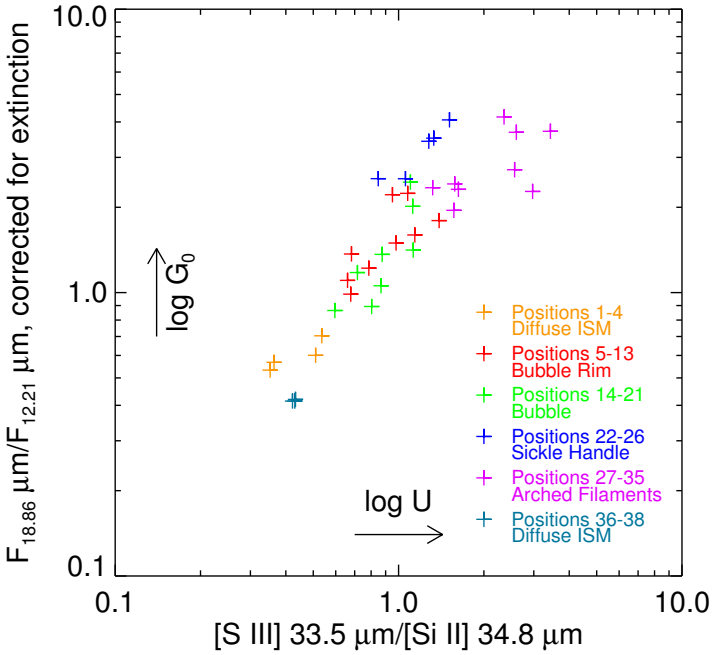

Fig. 3.— Relationship between the color temperature of the continuum and the ratio of intensities of the [S III] and [Si II] lines.

4. Summary

Thirty-eight positions were observed with Spitzer's IRS SH and LH modules in the Galactic Center. From the line spectra we have concluded that both shocks and photoionization excite the gas, and that the radiation field, although containing high energy photons, ranges from high intensity near the Arches Cluster to very low intensity ($U \sim -4$) at distances of several tens of pc from the Quintuplet Cluster. The variation in radiation field intensity is seen in both the amount and color temperature of the MIR continuum (12 – 35 μm) and in the relative strengths of the components of the 17 μm complex of PAH emission features. In the highest radiation fields, both the 16.4 and the 17.4 μm features are weak to non-existent, the 16.4 μm feature appears in medium intensity radiation fields, and the 16.4 and 17.4 μm features are both strong in low intensity but still ionizing radiation fields. The PAH features from 11 – 15 μm do not vary over this range of radiation field intensity.

This work is based on observations made with the *Spitzer Space Telescope*, which is operated by the Jet Propulsion Laboratory, California Institute of Technology, under a contract with NASA. Support for this work was provided by NASA. The IRS was a collaborative ven-

ture between Cornell University and Ball Aerospace Corporation funded by NASA through the Jet Propulsion Laboratory and Ames Research Center. JPS acknowledges support from NASA/Ames Research Center Research Interchange Grant NNA05CS33A to the SETI Institute.

REFERENCES

Draine, B. T., & Li, A. 2007, ApJ, 657, 810

Hony, S., et al. 2001, A&A, 370, 1030

Houck, J. R., et al. 2004, ApJS, 154, 18

Hudgins, D. M., & Allamandola, L. J. 1999, ApJ, 516, L41

Peeters, E., et al. 2002, A&A, 390, 1089

Peeters, E., Allamandola, L. J., Hudgins, D. M., Hony, S., & Tielens, A. G. G. M. 2004a, in ASP Conf. Ser. 309, Astrophysics of Dust, ed. A. N. Witt, G. C. Clayton, & B. T. Draine (San Francisco: ASP), 141

Peeters, E., Mattioda, A. L., Hudgins, D. M., & Allamandola, L. J. 2004b, ApJ, 617, L65

Sellgren, K., Uchida, K. I., & Werner, M. W. 2007, ApJ, 659, 1338

Simpson, J. P., Colgan, S. W. J., Cotera, A. S., Erickson, E. F., Hollenbach, D. J., Kaufman, M. J., & Rubin, R. H. 2007, ApJ, 670, 1115

Simpson, J. P., Witteborn, F. C., Cohen, M., & Price, S. D. 1999, in ASP Conf. Ser. 186, The Central Parsecs of the Galaxy, ed. H. Falke, A. Cotera, W. J. Duschl, F. Melia, & M. J. Rieke, (San Franscisco: ASP), 527

Smith, J. D. T., et al. 2007, PASP, 119, 1113

van Diedenhoven, B., et al. 2004, ApJ, 611, 928

Werner, M. W., et al. 2004, ApJS, 154, 1

Yusef-Zadeh, F., & Morris, M. 1987, ApJ, 320, 545

This preprint was prepared with the AAS LaTeX macros v5.2.